Available online at www.sciencedirect.com

SCIENCE DIRECT®

Journal of Solid State Chemistry 179 (2006) 175–185

JOURNAL OF SOLID STATE CHEMISTRY

www.elsevier.com/locate/jssc

# Syntheses and crystal structures of a series of new divalent metal phosphonates with imino-bis(methylphosphonic acid)

Bing-Ping Yang[a], Andrey V. Prosvirin[b], Han-Hua Zhao[b], Jiang-Gao Mao[a,*]

[a]State Key Laboratory of Structural Chemistry, Fujian Institute of Research on the Structure of Matter, The Chinese Academy of Sciences, Fuzhou 350002, PR China
[b]Department of Chemistry, Texas A&M University, P.O. Box 30012, College Station, TX 77843-3012, USA

Received 18 July 2005; received in revised form 30 September 2005; accepted 16 October 2005
Available online 15 November 2005

## Abstract

Hydrothermal reactions of divalent transition metal salts with imino-bis(methylphosphonic acid), $NH(CH_2PO_3H_2)_2$ ($H_4L$) afforded three new metal phosphonates, namely, $Cu[NH(CH_2PO_3H)_2]$ **1**, $\{Co[NH_2(CH_2PO_3H)(CH_2PO_3)](H_2O)_2\}\cdot H_2O$ **2** and $Mn[NH_2(CH_2PO_3H)(CH_2PO_3)](H_2O)$ **3**. When $HO_2C(CH_2)_3N(CH_2PO_3H_2)_2$ was used as the phosphonate ligand and 4,4′-bipy as the second metal linker, $\{Cu_4[NH(CH_2PO_3)_2]_2(4,4'\text{-bipy})(H_2O)_4\}\cdot 9H_2O$ **4** with a pillared layered architecture was obtained. The $NH(CH_2PO_3)_2$ anion resulted from the cleavage of the $HO_2C(CH_2)_3$-group during the reaction. Although compounds **1**–**3** have a same $M/L$ ratio (1:1), they exhibit totally different structures.Compound **1** has a linear chain structure, in which each pair of square-pyramidal coordinated copper(II) ions are bridged by two phosphonate oxygen atoms to form a $Cu_2O_2$ dimeric unit, and such dimeric units are further interconnected via phosphonate groups to form a [010] chain. Compound **2** has a layered architecture built from $CoO_6$ octahedra bridged by phosphonate ligands. In compound **3**, the interconnection of the manganese(II) ions by bridging imino-diphosphonate ligands leads to a 3D network. Compound **4** has a pillar-layered structure, the layers composed of Cu(II) ions bridged by aminodiphosphonate ligands are interconnected by 4,4′-bipy ligands to form channels along *c*-axis. Several factors that affect the structures of the metal phosphonates formed have also been discussed. Compounds **2** and **3** show predominant antiferromagnetic interactions between magnetic centers.

*Keywords:* Hydrothermal syntheses; Crystal structures; Metal diphosphonates; Inorganic–organic hybrids; Magnetic properties

## 1. Introduction

A great number of metal phosphonates have been studied in the past decades due to their potential applications in the areas of catalysis, ion exchange, proton conductivity, intercalation chemistry, photochemistry, and materials chemistry [1]. Hydrothermal synthesis has been proved to be a very useful technique in the preparation of highly stable, infinite metal-ligand solids exhibiting many interesting properties [2]. Materials with open-framework and microporous structures are expected to find use as hybrid composite materials in electro–optical and sensing applications in the future [1,3]. Many of the metal phosphonates exhibit a variety of open frameworks such as layered and microporous structures. Attaching additional functional groups such as carboxylate groups, amino, hydroxyl, or crown ethers to the phosphonic acid have been proved to be very useful methods in building open-framework and microporous structures. A series of open framework compounds of $H_2O_3PCH_2CO_2H$ and $H_2O_3PCH_2CH_2CO_2H$ have been isolated mainly by the Ferey, Bujoli, Cheetham and Sevov groups [3–7]. A number of porous metal phosphonates with crown ether moieties have been recently reported [8]. Results of our research and others indicate that amino-carboxylic-phosphonic acids are also capable of forming open framework structures with metal ions [4,9,10,15]. Phosphonate ligands with two phosphonic acid groups attached to a diamine group such as $R(NHCH_2PO_3H_2)_2$ are able to form metal

---

*Corresponding author. Fax: +86 591 8371 4946.
*E-mail address:* mjg@ms.fjirsm.ac.cn (J.-G. Mao).

0022-4596/$ - see front matter © 2005 Elsevier Inc. All rights reserved.
doi:10.1016/j.jssc.2005.10.015

compounds with a variety of structural types, such as mononuclear chelating compounds, 1D, 2D and 3D pillared layered structures [11]. A series of metal phosphonates with $R\text{N}(\text{CH}_2\text{PO}_3\text{H}_2)_2$ ($R$ = Me-, Et-, i-Bu-, $C_6H_5$-, $CH_3$-$C_6H_4$-, etc.) have been synthesized by our group as well as others, and results indicate that the substitute group $R$ plays a subtle role in the structures of the metal phosphonates [12,13]. Several divalent metal phosphonates with parent $\text{HN}(\text{CH}_2\text{PO}_3\text{H}_2)_2$ have been reported, such as $M[\text{NH}_2(\text{CH}_2\text{PO}_3\text{H})_2]_2(\text{H}_2\text{O})_2$ ($M$ = Mn, Co) [14,16c], $M_3[\text{NH}_2(\text{CH}_2\text{PO}_3)_2]_2$ ($M$ = Co, Cu) [15,16], with an $M/L$ ratio of 3:2, $\text{Pb}[\text{NH}(\text{CH}_2\text{PO}_3\text{H})_2]$ [17] and $\text{Pb}_2[\text{NH}(\text{CH}_2\text{PO}_3)_2]\cdot 2\text{H}_2\text{O}$ [18]. The aim of our current study is to investigate the effects of reaction conditions, such as pH value and the use of a second ligand on the structures of compounds thus formed. We deem that the different protonation modes of the ligand as well as the coordination number of the metal ion have a dramatic influence on the coordination mode adopted by the phosphonate ligand, and subsequently the structure of the metal phosphonates formed. It is also hoped that the second metal linker such as 4,4′-bipyridine could interconnect two metal phosphonate layers into a porous pillared layered structure. Our research efforts in this aspect lead to four new divalent metal phosphonates with $\text{HN}(\text{CH}_2\text{PO}_3\text{H}_2)_2$, namely, 1D $\text{Cu}[\text{NH}(\text{CH}_2\text{PO}_3\text{H})_2]$ **1**, 2D $\{\text{Co}[\text{NH}_2(\text{CH}_2\text{PO}_3\text{H})(\text{CH}_2\text{PO}_3)](\text{H}_2\text{O})_2\}\cdot\text{H}_2\text{O}$ **2**, 3D $\text{Mn}[\text{NH}_2(\text{CH}_2\text{PO}_3\text{H})(\text{CH}_2\text{PO}_3)](\text{H}_2\text{O})$ **3**, and $\{\text{Cu}_4[\text{NH}(\text{CH}_2\text{PO}_3)_2]_2(4,4'\text{-bipy})(\text{H}_2\text{O})_4\}\cdot 9\text{H}_2\text{O}$ **4** with a pillared layered architecture. Herein we report their syntheses, crystal structures, and magnetic properties.

## 2. Experimental section

### 2.1. Materials and instrumentation

The aminocarboxylate phosphonate ligand, *N*,*N*′-bis(phosphonomethyl)-amino-butyric acid $[\text{HO}_2\text{C}(\text{CH}_2)_3\text{N}(\text{CH}_2\text{PO}_3\text{H}_2)_2]$ was synthesized by a Mannich-type reaction according to procedures described previously [18]. All other chemicals were used as received without further purification. Elemental analyses were performed on a German Elementary Vario EL III instrument. X-ray powder diffraction (XRD) patterns (Cu*K*α) were collected in a sealed glass capillary on an XPERT-MPD $\theta-2\theta$ diffractometer. The FT-IR spectra were recorded on a Nicolet Magna 750 FT-IR spectrometer using KBr pellets in the range of $4000-400\,\text{cm}^{-1}$. Magnetic susceptibility measurements for compounds **2** and **3** were carried out on a Quantum Design PPMS at a magnetic field of 1000 G in the range of 2–300 K. Magnetic measurements for compounds **1** and **4** were not performed due to insufficient samples available. The raw data were corrected for the susceptibility of the container and the diamagnetic contributions of the sample using Pascal's constants. Thermogravimetric analyses were performed on an NETZSCH STA 449C unit, at a heating rate of 15 °C/min under a nitrogen atmosphere.

### 2.2. Synthesis

#### 2.2.1. Synthesis of $Cu[NH(CH_2PO_3H)_2]$ 1

A mixture of copper(II) acetate (100 mg, 0.5 mmol), $\text{HN}(\text{CH}_2\text{PO}_3\text{H}_2)_2$ (102.5 mg, 0.5 mmol), squaric acid ($\text{C}_4\text{H}_2\text{O}_4$) (28.5 mg, 0.25 mmol) and distilled water (10 mL) with an initial pH value of 2.0 was put into a Parr Teflon-lined autoclave (25 mL) and heated at 140 °C for 5 days. Blue cubic crystals of compound **1** were collected in a ca. 41% yield (55 mg) based on Cu. Without addition of the squaric acid, only $\text{Cu}_3[\text{NH}_2(\text{CH}_2\text{PO}_3)_2]_2$ was obtained. *Anal.* Found: C, 8.95%; H, 2.71%; N, 5.22%. Calc. for $\text{C}_2\text{H}_7\text{CuNO}_6\text{P}_2$ (Mr = 266.57): C, 9.0%; H, 2.65%; N, 5.25%. IR data (KBr): $3223\,\text{cm}^{-1}$ $\{\nu(\text{O–H})\}$; $1626\,\text{cm}^{-1}$ $\{\delta(\text{N–H})\}$; 1138 (s), 1078 (s) $\text{cm}^{-1}$ $\{\nu_{as}(\text{PO}_3)\}$; 1026, $926\,\text{cm}^{-1}$ $\{\nu_s(\text{PO}_3)\}$.

#### 2.2.2. Synthesis of $\{Co[NH_2(CH_2PO_3H)(CH_2PO_3)](H_2O)_2\}\cdot H_2O$ 2

Hydrothermal reaction of a mixture of cobalt(II) sulfate (77.5 mg, 0.5 mmol), $\text{HN}(\text{CH}_2\text{PO}_3\text{H}_2)_2$ (102.5 mg, 0.5 mmol) and distilled water (10 mL) with the pH pre-adjusted to ~2.0 by addition of 0.25 mmol 4,4′-bipy (39 mg) in a Teflon-lined autoclave (25 mL) at 130 °C for 5 days resulted in the purple lamellar crystals of compound **2** as a single phase material in a yield of 46% based on Co. Compound **2** can also be prepared by using the cobalt chloride or cobalt nitrate as cobalt(II) sources. *Anal.* Found: C, 7.55%; H, 4.31%; N, 4.35%. Calc. for $\text{C}_2\text{H}_{13}\text{CoNO}_9\text{P}_2$ (Mr = 316.01): C, 7.60%; H, 4.15%; N, 4.43%. IR data (KBr): $3417\,\text{cm}^{-1}$ $\{\nu_s(\text{O–H})\}$; $1660\,\text{cm}^{-1}$ $\{\delta(\text{N–H})\}$; 1188, $1105\,\text{cm}^{-1}$ $\{\nu_{as}(\text{PO}_3)\}$; 985, $931\,\text{cm}^{-1}$ $\{\nu_s(\text{PO}_3)\}$.

#### 2.2.3. Synthesis of $Mn[NH_2(CH_2PO_3H)(CH_2PO_3)](H_2O)$ 3

$\text{MnSO}_4$ (75.5 mg, 0.5 mmol), $\text{HN}(\text{CH}_2\text{PO}_3\text{H}_2)_2$ (102.5 mg, 0.5 mmol) and distilled water (10 mL) were mixed and the pH was adjusted to ~2.0 by addition of 0.25 mmol 4,4′-bipy (39 mg). The resultant solution was put into a Teflon-lined stainless steel autoclave (25 mL) and heated at 140 °C for 5 days. Colorless brick-shaped crystals of **3** were collected in ca. 65% yield (90 mg). $\text{C}_2\text{H}_9\text{MnNO}_7\text{P}_2$ (Mr = 275.98) C, 8.70%; H, 3.29%; N, 5.08%; found: C, 8.59%; H, 3.33%; N, 4.95%. IR data (KBr): $3161\,\text{cm}^{-1}$ $\{\nu_s(\text{O–H})\}$; $1578\,\text{cm}^{-1}$ $\{\delta(\text{N–H})\}$; 1119, $1074\,\text{cm}^{-1}$ $\{\nu_{as}(\text{PO}_3)\}$; 987, $926\,\text{cm}^{-1}$ $\{\nu_s(\text{PO}_3)\}$.

#### 2.2.4. Synthesis of $\{Cu_4[NH(CH_2PO_3)_2]_2(4,4'\text{-}bipy)(H_2O)_4\}$ $9H_2O_4$

A mixture of copper(II) nitrate (120.8 mg, 0.5 mmol), $\text{HOOC}(\text{CH}_2)_3\text{N}(\text{CH}_2\text{PO}_3\text{H}_2)_2$ (145.6 mg, 0.5 mmol), 4,4′-bipy (39 mg, 0.25 mmol) and distilled water (10 mL) with an initial pH value of 2.0 was put into a Parr Teflon-lined autoclave and heated at 140 °C for 5 days. No solids were isolated. The resulted blue solution with pH value of 5.0 was allowed to evaporate very slowly at room temperature. After 2 months, 5 mg of blue plate crystals of compound

Table 1
Summary of crystal data and structural refinements for compounds **1**–**4**

| Compound | **1** | **2** | **3** | **4** |
|---|---|---|---|---|
| Empirical formula | $C_2H_7CuNO_6P_2$ | $C_2H_{13}CoNO_9P_2$ | $C_2H_9MnNO_7P_2$ | $C_{14}H_{44}Cu_4N_4O_{25}P_4$ |
| Fw | 266.57 | 316.00 | 275.98 | 1046.57 |
| Space group | $P2_{1/n}$ | $P2_{1/c}$ | $Cc$ | $Fdd2$ |
| $a$, Å | 8.819(1) | 8.7876(6) | 6.748(1) | 15.4398(8) |
| $b$, Å | 7.403(1) | 7.2981(4) | 8.865(2) | 52.022(3) |
| $c$, Å | 11.168(2) | 15.6325(8) | 12.988(3) | 11.2107(7) |
| $\beta$, ° | 97.991(2) | 90.266(2) | 95.569(3) | 90 |
| $V$, Å$^3$ | 722.0(2) | 1002.5(1) | 773.3(3) | 9004.5(9) |
| $Z$ | 4 | 4 | 4 | 8 |
| $D_{\mathrm{calcd}}$, g/cm$^3$ | 2.452 | 2.094 | 2.371 | 1.544 |
| Temp, K | 293(2) | 293(2) | 293(2) | 293(2) |
| $\mu$, mm$^{-1}$ | 3.458 | 2.064 | 2.129 | 2.082 |
| GOF | 1.104 | 1.128 | 1.087 | 1.119 |
| $R1, wR_2[I>2\sigma(I)]$ | 0.0322, 0.0807 | 0.0776, 0.1918 | 0.0276, 0.0738 | 0.0625, 0.1411 |
| $R1, wR_2$(alldata) | 0.0354, 0.0840 | 0.0987, 0.2134 | 0.0276, 0.0739 | 0.0858, 0.1561 |

$R1 = \sum(|F_o| - |F_c|)/\sum|F_o|$; $wR2 = \left[\sum w(|F_o| - |F_c|)^2/\sum wF_o^2\right]^{1/2}$

**4** were collected in a low yield of ~4%. The butyric acid moiety of the diphosphonate ligand was cleaved during the reaction. Effects to enhance the yield by direct using $HN(CH_2PO_3H_2)_2$ as phosphonate ligand were tried, but only $Cu_3[NH_2(CH_2PO_3)_2]_2$ was obtained. IR data (KBr): 3394 cm$^{-1}$ $\{v_s(O–H)\}$; 1616 cm$^{-1}$ $\{\delta(N–H)\}$; 1086, 1047 cm$^{-1}$ $\{v_{as}(PO_3)\}$; 989 cm$^{-1}$ $\{v_s(PO_3)\}$.

### 2.3. X-ray crystallography

Data collections were performed on a Siemens Smart CCD diffractometer, using graphite-monochromated Mo*K*α radiation ($\lambda = 0.71073$ Å). Intensity data were collected by using narrow frame method with 0.3° per frame in $\varphi$ at 293 K. A total of 1265 (for **1**), 1726 (for **2**), 835 (for **3**) or 3449 (for **4**) independent reflections were collected among which 1187(for **1**), 1433(for **2**), 833 (for **3**) or 2783 (for **4**) with $I > 2.0\sigma(I)$ were considered observed. Absorption corrections were performed by using the SADABS program [19]. All four structures were solved by direct methods and refined by full-matrix least-squares fitting on $F^2$ by SHEXLS [20]. All of the non–hydrogen atoms were refined anisotropically. For compound **4**, O(6W) and O(6w′) with a short O–O distance of 2.11(8) Å are considered to be two orientations of a disordered water molecule and each refined with 50% occupancy. O(7w) is also disordered with O(7w)···O(7w) (symmetry code: $-x$, $-y$, $-z$) separation of 2.34(8) Å and its occupancy is reduced to 50%. O(5w) and O(8w) with large thermal parameters were also refined with 50% occupancy. These five atoms were refined isotropically. All hydrogen atoms were located at geometrically calculated positions and refined with isotropic thermal parameters. The hydrogen atoms for the water molecules in compound **4** were not included in the refinements. A summary of the crystallographic data for four compounds is listed in Table 1. Selected bond distances for four compounds are given in Table 2.

CCDC Nos. 246367–246370 contain the supplementary crystallographic data for this paper. These data can be obtained free of charge at www.ccdc.cam.ac.uk/conts/retrieving.html [or from the Cambridge Crystallographic Data Centre, 12, Union Road, Cambridge CB2 1EZ, UK; fax: (internat.) +44-1223/336-033; E-mail: deposit@ccdc.cam.ac.uk].

## 3. Results and discussion

Compounds **1**–**4** feature four different types of structures. It is worthy to discuss the synthetic conditions for compounds **1**–**4**. Compounds **1**–**3** were obtained in acidic media (pH = 2.0). Under such condition the amine group and one of the phosphonate group of the phosphonate ligand are protonated. With less acidic condition (pH = 5) and addition of 4,4′-bipy, all protons are removed and the phosphonate ligand carries more negative charges, which led to the formation of compound **4**. Hence, pH value of the reaction media has an strong effect on the compositions and structures of the metal phosphonates isolated. $M/L$ ratio also has some influence on the structure of metal compounds thus formed. In our experiments, the $M/L$ ratio of starting materials is 1:1; hence, it is not surprising that compounds **1**–**3** has an $M/L$ ratio of 1:1. For compound **4**, the $NH(CH_2PO_3H_2)_2$ ligand came from the decomposing of $HOOC(CH_2)_3N$-$(CH_2PO_3H_2)_2$, the $M/L$ of 2:1 in compound **4** is probably owing to the incompleteness of the ligand conversion. When iminobis(methylphosphonic acid) was used as the starting material, only $Cu_3[NH_2(CH_2PO_3)_2]_2$ was obtained. $Cu_3[NH_2(CH_2PO_3)_2]_2$ itself was initially prepared by reaction of copper(II) chloride with nitrilotris(methylene)-triphosphonic acid, one $H_2O_3PCH_2$-moiety was cleaved

Table 2
Selected bond lengths (Å) for compounds **1**–**4**

| | | | |
|---|---|---|---|
| *Compound* **1** | | | |
| Cu(1)–O(11) | 1.936(3) | Cu(1)–N(1) | 2.007(3) |
| Cu(1)–O(21)#1 | 1.967(3) | Cu(1)–O(13)#2 | 2.268(3) |
| Cu(1)–O(21) | 1.999(3) | Cu(1)–Cu(1)#1 | 3.0370(9) |
| O(21)···O(21)#1 | 2.551(5) | O(23)···O(22)#3 | 2.457(4) |
| *Compound* **2** | | | |
| Co(1)–O(22) | 2.062(6) | Co(1)–O(13)#3 | 2.121(6) |
| Co(1)–O(23)#1 | 2.063(6) | Co(1)–O(1W) | 2.135(6) |
| Co(1)–O(12)#2 | 2.087(6) | Co(1)–O(2W) | 2.150(6) |
| O(11)···O(21)#4 | 2.621(8) | O(11)-H(11a)···O(21)#4 | 170.8° |
| O(3W)···O(1W)#5 | 2.804(10) | O(3W)···O(21)#6 | 2.856(10) |
| *Compound* **3** | | | |
| Mn(1)–O(22) | 2.129(4) | Mn(1)–O(11)#3 | 2.241(4) |
| Mn(1)–O(23)#1 | 2.133(4) | Mn(1)–O(13) | 2.242(4) |
| Mn(1)–O(12)#2 | 2.174(4) | Mn(1)–O(1W) | 2.265(4) |
| *Compound* **4** | | | |
| Cu(1)–O(12) | 1.960(8) | Cu(2)–O(21)#2 | 1.921(7) |
| Cu(1)–O(23) | 1.981(8) | Cu(2)–O(22)#3 | 1.959(8) |
| Cu(1)–N(2) | 1.998(7) | Cu(2)–O(13) | 1.968(8) |
| Cu(1)–N(1) | 2.026(7) | Cu(2)–O(2W) | 2.002(6) |
| Cu(1)–O(11)#1 | 2.219(8) | Cu(2)–O(1W) | 2.333(8) |
| O(1w)···O(3w) | 2.85(2) | O(1w)···O(4w) | 2.77(2) |
| O(3w)···O(7w) | 2.89(5) | O(4w)···O(5w) | 2.97(4) |
| O(4w)···O(6w′) | 2.89(6) | O(3w)···O(8w) | 3.04(8) |
| O(5w)···O(8w)#4 | 2.83(8) | O(2w)···O(6w)#5 | 2.83(4) |

Symmetry transformations used to generate equivalent atoms:
For **1**: #1 $-x+2, -y, -z+2$ ♯2 $-x+2, -y+1, -z+2$ ♯3 $-x+3/2, y-1/2, -z+5/2$.
For **2**: #1 $-x+1, y-1/2, -z+3/2$ ♯2 $-x+1, -y+1, -z+2$ ♯3 $x, y-1, z$ ♯4 $x, -y+3/2, z+1/2$ ♯5 $-x+1, y+1/2, -z+3/2$ ♯6 $-x, y+1/2, -z+3/2$.
For **3**: ♯1 $x, -y, z+1/2$ ♯2 $x-1/2, y-1/2, z$ ♯3 $x-1, y, z$.
For **4**: ♯1 $x+1/4, -y+1/4, z+1/4$ ♯2 $x+1/4, -y+1/4, z-3/4$ ♯3 $x, y, z-1$ ♯4 $-1/2-x, y, 1/2+z$ ♯5 $-1/4+x, 1/4-y, -1/4+z$.

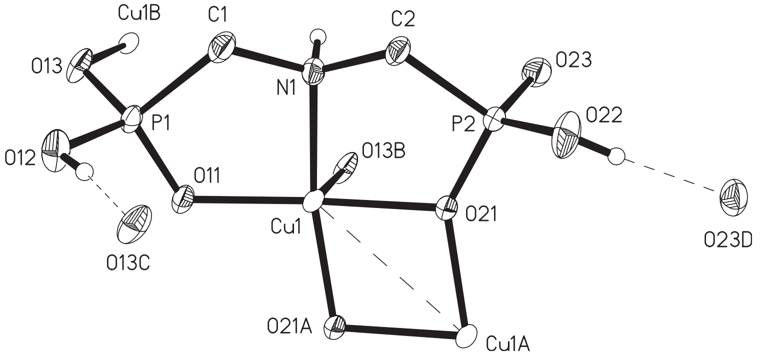

Fig. 1. ORTEP representation of the selected unit of compound **1**. Thermal ellipsoids are drawn at a 50% probability level.

during the reaction [16a]. Reaction of copper(II) acetate, $HN(CH_2PO_3H_2)_2$ and squaric acid lead to the formation of $Cu[NH(CH_2PO_3H)_2]$. The squaric acid acts only as a pH mediator, as does the 4,4′-bipyridine in the preparation of compounds **2** and **3**.

The structure of compound **1** features 1D chains built from $Cu_2O_2$ units interconnected by phosphonate groups (Fig. 1). As shown in Fig. 1, the Cu(II) ion is 5-coordinated by a tridentate chelating $H_2L$ dianion (O(11), O(21) and N(1)), and two phosphonate oxygen atoms (O(21) and O(13)) from two other phosphonate ligands. The coordination geometry around the copper(II) ion can be best described as a "Jahn Teller" distorted square-pyramid with the axial bond elongated. The copper(II) ion is slightly away (0.14 Å) from the square plane formed by O(11), N(1), O(21), O(21a). These Cu–O (1.936(3)–1.999(3) Å) and Cu–N (2.007(3) Å) distances are significantly shorter than the axial Cu–O bond (2.268(3) Å). This type of coordination geometry is different from those reported in $Cu_3[NH_2(CH_2PO_3)_2]_2$ with an $M/L$ ratio of 3:2, in which the copper(II) ions are in octahedral or tetrahedral environment [16]. The $H_2L$ dianion acts as a pentadentate ligand, it chelates with one copper(II) ion tridentately (O(11), O(21) and N(1)), and also bridges with two other Cu(II) ions. O(21) is a bidentate metal linker. Based on charge balance and P–O bond distances, both phosphonate groups are 1H-protonated. This type of coordination mode is different from that in $Cu_3[NH_2(CH_2PO_3)_2]_2$, in which both phosphonate groups of the 3-charged phopsphonate anion are completely deprotonated, and the phosphonate ligand is heptadentate (chelating with a metal ion bidentately and bridging with five other metal ions), also the amine group in the latter compound is protonated and non-coordinated [16]. Each pair of Cu(II) ions are bridged by two bidentate phosphonate oxygen atoms (O(21) and O(21a)) to form a planar $Cu_2O_2$ unit with Cu–Cu separation of 3.037(1) Å. These $Cu_2O_2$ dimeric units are further interconnected by bridging phosphonate ligands into a 1D chain along *b*-axis (Fig. 2). The Cu–Cu distance between two Cu(II) ions bridged by a phosphonate group (Cu–O–P–O–Cu) is 4.612(1) Å. Neighboring chains are interlinked via strong O(22)–H(22a)⋯O(23) (symmetry code: $-x+3/2,\ y-1/2,\ -z+5/2$) hydrogen bonds into a (101) 2D layer (Fig. 2). The hydrogen bond length and angle are 2.457(4) Å and 151.9°, respectively. Such layers are further cross-linked by O(12)-H(12a)⋯O(13) (symmetry code: $-x+3/2,\ y-1/2,\ -z+3/2$) hydrogen bonds into a 3D network (Fig. 3). The O(12)–H(12a)⋯O(13) bond length and angle are 2.591(4) Å and 172.4°, respectively.

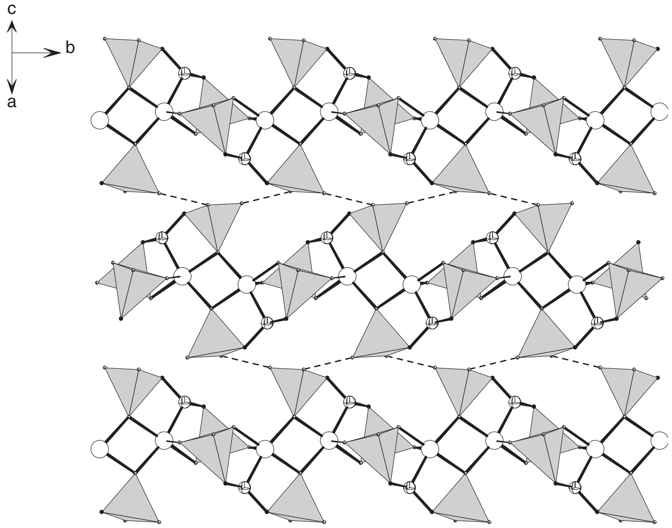

Fig. 2. A ⟨1 0 1⟩ layer composed of 1D chain of copper(II) diphosphonate interconnected by hydrogen bonds in **1**. The C–$PO_3$ tetrahedra are graded in light gray. Cu and N atoms are represented by open and octand circles, respectively.

Compound **2** with a layered structure is the third cobalt(II) compound with this phosphonate ligand. The other two compounds reported are one-dimensional $Co[NH(CH_2PO_3H)_2]_2(H_2O)_2$ ($M/L = 1{:}2$) and three-dimensional $Co_3[NH_2(CH_2PO_3)_2]_2$ with a 3:2 $M/L$ ratio [14–16]. As shown in Fig. 4, the asymmetric unit of compound **2** consists of one Co(II) ion, one $[H_2L]^{2-}$ anion, two aqua ligands and one lattice water molecule. The Co(II) ion is octahedrally coordinated by four phosphonate oxygen atoms from four diphosphonate ligands and two aqua ligands. The Co–O bond lengths range from 2.062(6) to 2.150(6) Å, which are comparable to those reported in other cobalt(II) phosphonates [5,6,14,15]. The phosphonate ligand adopts a different coordination mode from those in the Co(II) compounds previously reported [14,15]. Each amino-diphosphonate ligand is tetradentate and bridges with four cobalt(II) ions. All four coordination phosphonate oxygen atoms (O(12), O(13), O(22) and O(23)) are in a monodentate fashion. Two phosphonate oxygen atoms (O(11) and O(21)) are non-coordinated. Based on P–O distances as well as the coordination mode of the phosphonate ligand, O(11) is 1H-protonated. The nitrogen atom is also protonated. It is worthy to mention the coordination modes of this phosphonate ligand in other Co(II) compounds. The phosphonate ligand in

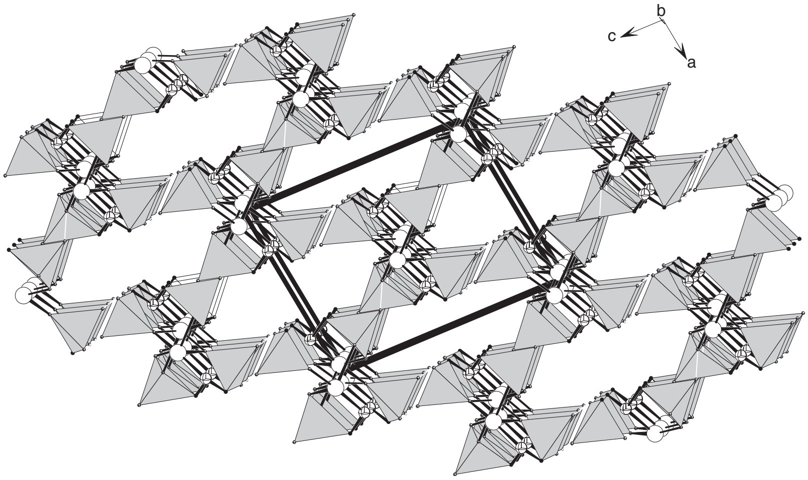

Fig. 3. A view of the crystal structure of **1** down the *b* axis. The C–$PO_3$ tetrahedra are graded in light gray. Cu and N atoms are represented by open and octand circles, respectively.

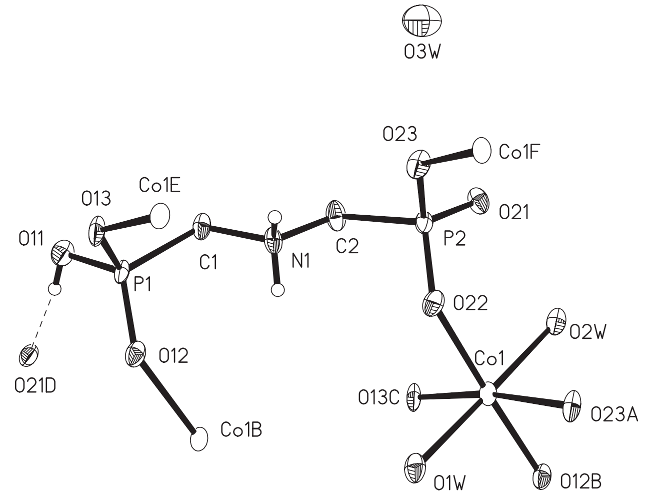

Fig. 4. An ORTEP representation of the selected unit in **2**. Thermal ellipsoids are drawn at 50% probability.

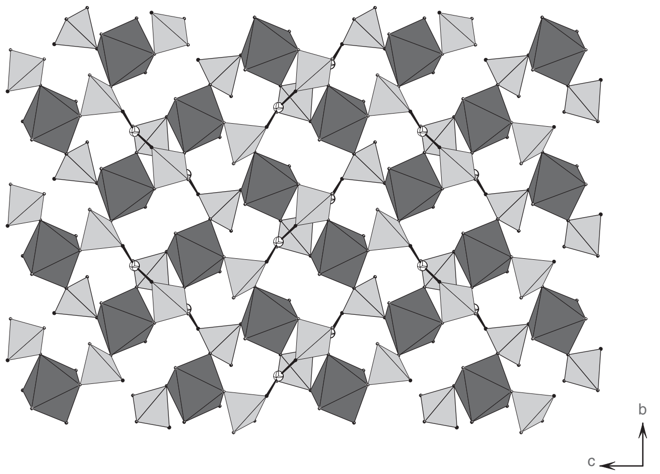

Fig. 5. A ⟨2 0 0⟩ layer of cobalt(II) diphosphonate in **2**. The C–$PO_3$ tetrahedra and $CoO_6$ octahedra are shaded in light and dark gray, respectively. N atoms are drawn as octand circles.

$Co[NH(CH_2PO_3H)_2]_2$ is bidentate bridging, both phosphonate groups and the nitrogen atom are singly protonated [14]. The phosphonate ligand in $Co_3[NH_2(CH_2PO_3)_2]_2$ is hexadentate and bridges with six Co(II) ions in a tetrahedral coordination geometry, and only the amine group is singly protonated [15].

The interconnection of Co(II) ions by bridging diphosphonate ligands resulted in a (200) layer (Fig. 5). Two types of rings are formed within the layer. The first type is the 8-membered ring composed of two cobalt(II) ions and two diphosphonate ligands, and the second one is the 6-membered ring formed by two cobalt(II) cations, a diphosphonate ligand and one phosphonate group.

The lattice water molecules are located in the middle of the interlayer space (Fig. 6), forming hydrogen bonds with the non-coordination phosphonate oxygen atoms as well as aqua ligands (Table 2). The inter layer distance is about 8.7 Å.

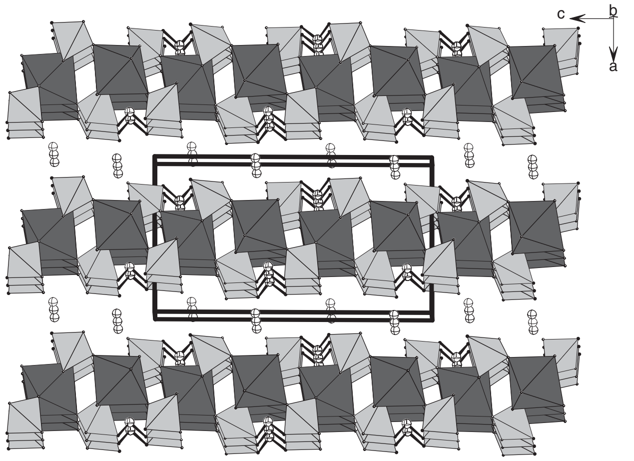

Fig. 6. A view of the crystal structure of **2** down the *b*-axis. The C–$PO_3$ tetrahedra and $CoO_6$ octahedra are shaded in light and dark gray, respectively. C and N atoms are represented by black and octand circles, respectively.

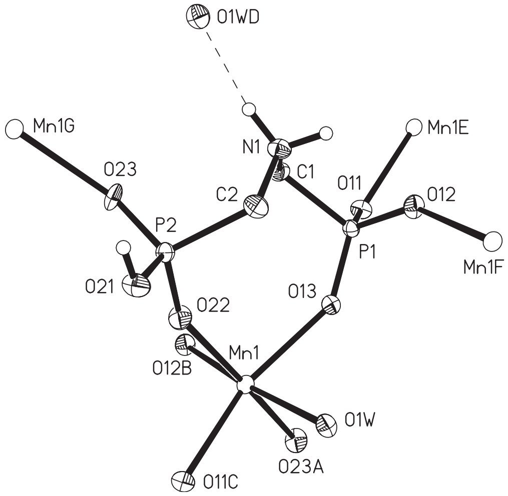

Fig. 7. ORTEP representation of the selected unit in **3**. Thermal ellipsoids are drawn at 50% probability.

Different from one-dimensional $Mn[NH_2(CH_2PO_3H)_2]_2(H_2O)_2$ [16c], compound **3** with a 1:1 $M/L$ ratio features a three-dimensional network structure. As shown in Fig. 7, the asymmetric unit of **3** contains one $Mn^{2+}$ ion, one $[H_2L]^{2-}$ dianion and an aqua ligand. The Mn(II) ion is octahedrally coordinated by a bidentate chelating diphosphonate anion [O(13) and O(22)], three phosphonate oxygen atoms from three other diphosphonate ligands as well as an aqua ligand. The Mn–O distances are in the range of 2.129(4)–2.265(4) Å (Table 2). These distances are comparable to those reported in $Mn[NH_2(CH_2PO_3H)_2]_2(H_2O)_2$ [16c]. The diphosphonate $H_2L$ ligand adopts a different coordination mode from those in **1** and **2** as well as that in $M[NH_2(CH_2PO_3H)_2]_2(H_2O)_2(M = Mn,\ Co)$ ([14,16c]). It acts as a pentadentate ligand. The phosphonate dianion chelates with a Mn(II) ion bidentately and also bridges with three other Mn(II) ions. O(21) is singly protonated and remains non-coordinated. The nitrogon atom is also protonated.

The interconnection of the manganese(II) ions via bridging diphosphonate ligands leads to a 3D network (Fig. 8) with small tunnels running along *a*-axis. The tunnel is formed by 8-membered rings composed of three Mn(II) ions, a diphosphonate anion and two phosphonate groups.

The structure of compound **4** features a pillared layered architecture. As shown in Fig. 9, there are two unique Cu(II) ions in the asymmetric unit of compound **4**. Cu(1) is five-coordinated by a phosphonate ligand in a tridentate chelating fashion (N(1), O(12) and O(23)), one phosphonate oxygen atom from a neighboring Cu(1)L unit and one nitrogen atom from a 4,4′-bipy ligand. The coordination geometry around Cu(1) is an axially elongated (Cu(1)–O(11a) 2.219(8) Å) square pyramid. The Cu(1)–O bond lengths fall between 1.960(8) and 2.219(8) Å, and Cu(1)–N bond lengths are in the range of 1.998(7)–2.026(7) Å. Cu(2) atom with a similar square pyramidal geometry is coordinated by three phosphonate oxygens from three Cu(1)L units and two aqua ligands. The axial Cu–O(O1w) bond length of 2.333(8) Å is significantly longer than the remaining Cu–O bonds. The O–Cu–O bond angles are in the range of 85.9(3)–175.1(4)°. These bond lengths and angles are comparable to those in compound **1** as well as those reported in $Cu_3[NH_2(CH_2PO_3)_2]_2$ [16]. The amino-diphosphonate ligand is heptadentate, chelating with a copper(II) tridentately and also bridging with four other Cu(II) ions [1Cu(1) + 3Cu(2)]. Each phosphonate oxygen atom is monodentate. The diphosphonate ligand is 4- in charge, that is all four acidic protons have been completely deprotonated. Such coordination mode is significantly different from that in compound **1** as well as in $Cu_3[NH_2(CH_2PO_3)_2]_2$ [16].

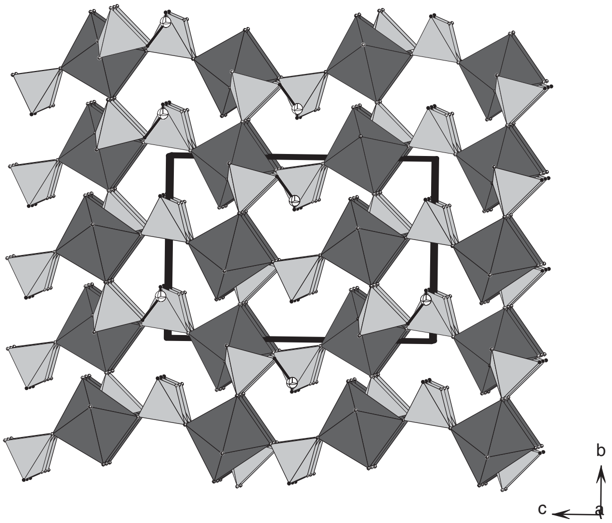

Fig. 8. View of the crystal structure of **3** down the *a*-axis. The C–$PO_3$ tetrahedra and $MnO_6$ octahedra are shaded in light and dark gray, respectively. N atoms are represented by octand circles, respectively.

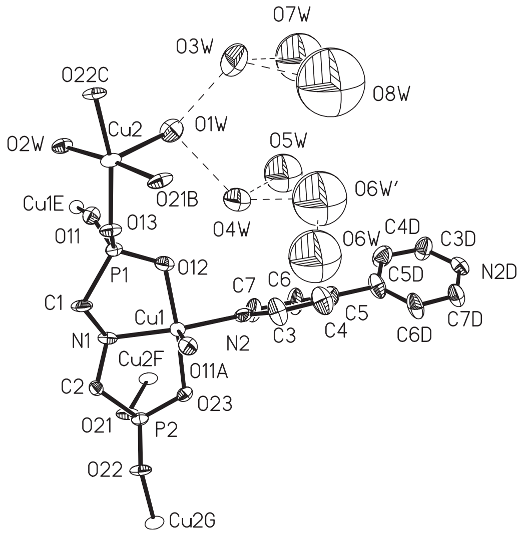

Fig. 9. ORTEP representation of the selected unit in **4**. Thermal ellipsoids are drawn at 50% probability. Hydrogen bonds are represented by dashed lines.

The above $CuN_2O_3$, $CuO_5$ polyhedra are interconnected by bridging imino-diphosphonate ligands into 2D layers normal to the *b*-axis (Fig. 10). Within the layer, 6-membered rings composed of three Cu(II) ions and three phosphonate groups are formed. The interlayer distance is about 13 Å (about *b*/4). These 2D layers are further cross-linked by the bidentate bridging 4,4′-bipy ligands to form a pillared-layered architecture (Fig. 11). The distance between two parallel pillar agents is about 7.6 Å (ca. *a*/2). The size of the cavity thus formed is about $5\times 7\,Å^2$ after the deduction of Van der Waals' radii for the related atoms. The lattice water molecules are located at the tunnels and are involved in extensive hydrogen bonding (Table 2). These lattice water molecules are interacted through hydrogen bonds with O⋯O contacts ranging from 2.83(8) to 3.04(8) Å. They are also hydrogen bonded to the aqua ligands of the inorganic framework with O⋯O separations in the range of 2.77(2)–2.85(2) Å (Table 2). The amount of void space can also be calculated by removing all lattice water molecules, and using the CALC SOLV command in PLATON [21]. The calculated void space value is 46.6%. When the lattice water molecules are included in the calculation, the void space becomes zero.

$NH(CH_2PO_3H_2)_2$ ($H_4L$) is a versatile ligand. The free ligand occurs in the zwitterion form (Scheme 1a). It is able to adopt a variety of coordination modes upon its reaction with metal salts, as shown in Scheme 1 and Ref. ([15,16c]). It is interesting to note that although compounds **1**–**3** have a same $M/L$ ratio of 1:1, but their structures and the coordination modes for the ligand are completely different. The diphosphonate ligand in $Cu[NH(CH_2PO_3H)_2]$ chelates with a copper(II) in a tridentate fashion, and also bridges with another metal ion (Scheme 1b). In compounds **2** and **3**, the amine group is protonated, one phosphonate group is 1H-protonated whereas the other one is completely

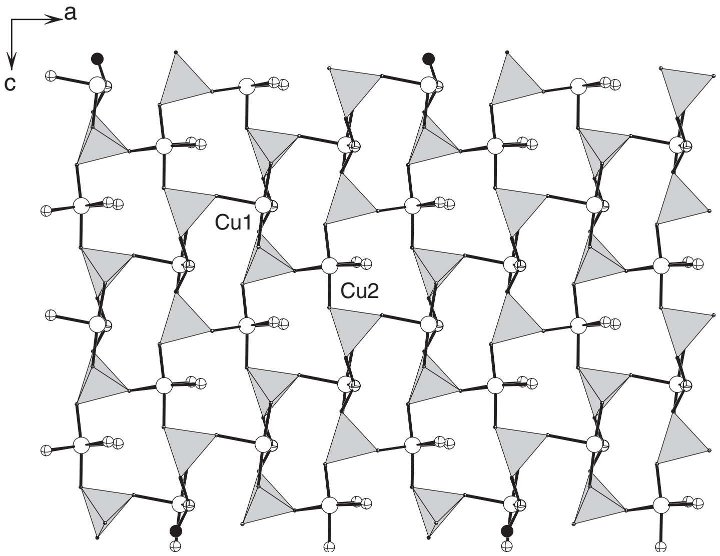

Fig. 10. A 2D layer of copper(II) diphosphonate in **4**. The C–$PO_3$ tetrahedra are graded in light gray. Cu, N and O atoms are represented by open, octand and crossed circles, respectively.

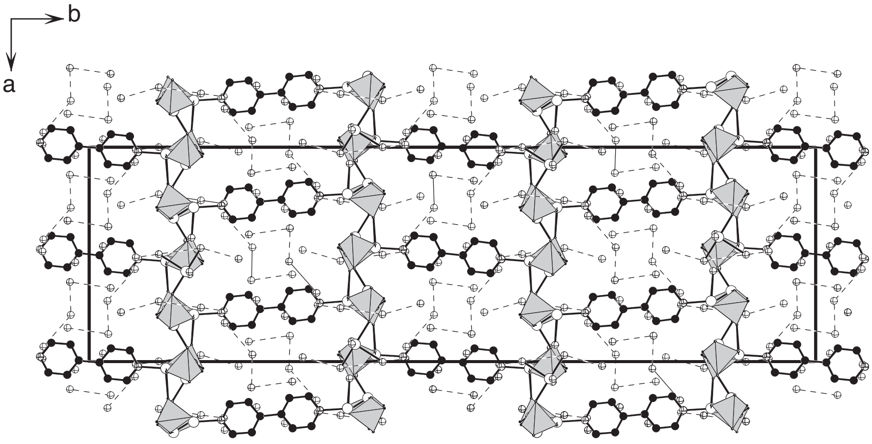

Fig. 11. View of the pillar-layered structure of **4** down the *c*-axis. The C–$PO_3$ tetrahedra are graded in light gray. Cu, N and O atoms are represented by open, octand and crossed circles, respectively. Hydrogen bonds are represented by dashed lines.

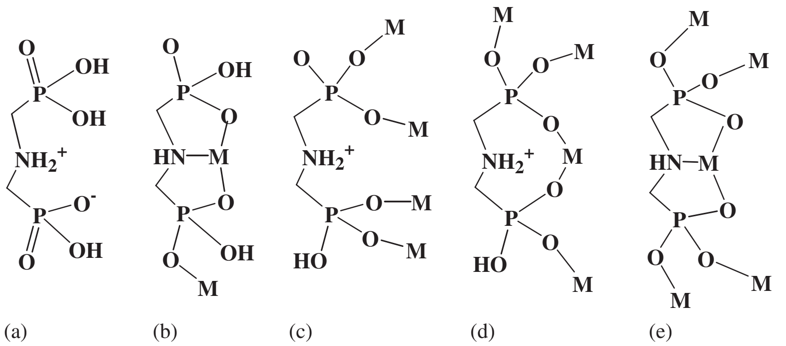

Scheme 1. $H_4L$ (a) and its coordination modes in compounds **1** (b), **2** (c), **3** (d) and **4** (e).

deprotonated (Scheme 1c and d). For compound **4**, the ligands have been fully deprotonated, all phosphonate oxygen atoms as well as the nitrogen atom are involved in metal coordination (Scheme 1e).

Compounds **1**–**3** can be obtained as single-phase products based on XRD studies.

The magnetic properties for compounds **2** and **3** have been also studied. Results are shown in Fig. 12. The

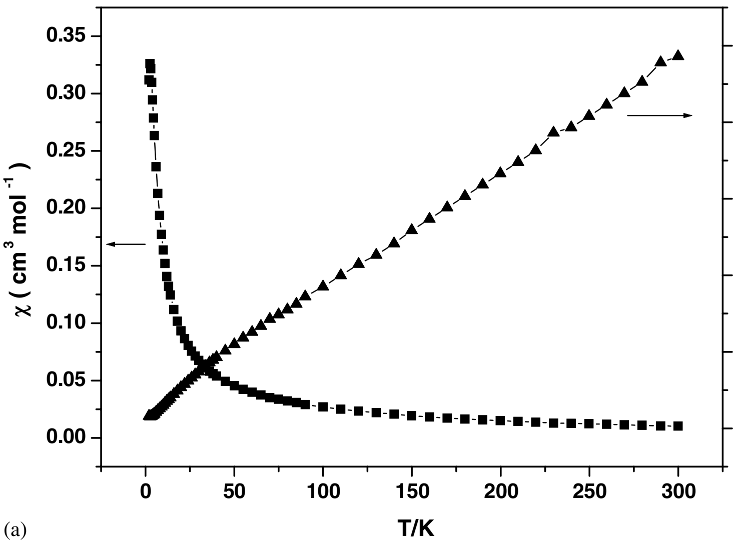

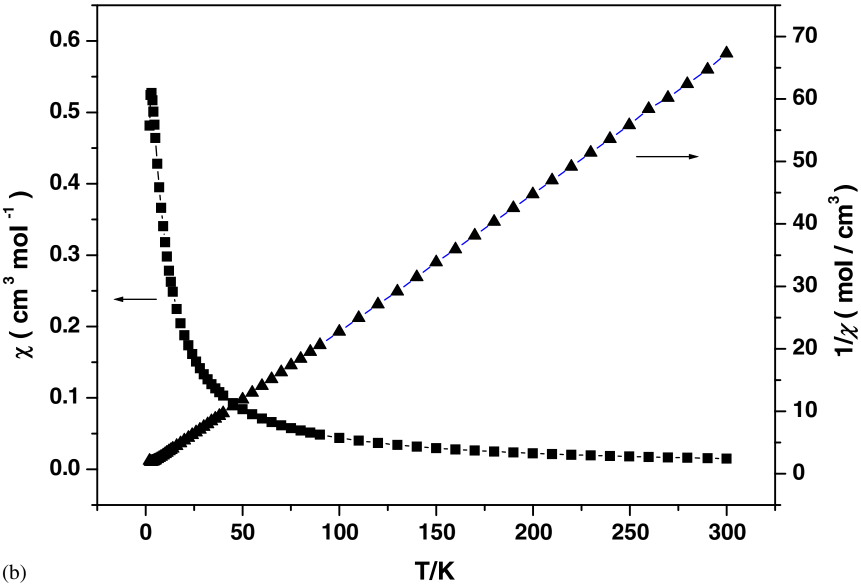

Fig. 12. Plots of $\chi_M$ and $1/\chi_M$ versus $T$ for compounds **2** (a) and **3** (b).

effective magnetic moment ($\mu_{\mathrm{eff}}$) at room temperature is $4.98\mu_{\mathrm{B}}$, which is much larger than the spin-only value of $3.87\mu_{\mathrm{B}}$ for an Co(II) ($S = 3/2$) center, due to the orbital contribution of the high spin cobalt(II) ion. At 2 K, $\mu_{\mathrm{eff}}$ is decreased to $2.233\mu_{\mathrm{B}}$, indicating the antiferromagnetic interaction between Co(II) centers. The antiferromagnetic exchange interactions between the Co(II) ions in **2** is also indicated by a maximum of $\chi_M$ at 2.5 K (Fig. 12a) and the negative Weiss constant ($\theta$) of –23.3 K obtained by fitting of the data by Curie–Weiss law in 50–300 K. The magnetic interaction in compound **2** is mainly from Co(II) ions bridged by phosphonate group within the 2D metal phosphonate layer (Co⋯Co separations of 5.298(1) and 5.483(1) Å), the interlayer Co(II)⋯Co(II) magnetic interaction is expected to be very small due to the larger Co⋯Co separation (8.788(1) Å). Compound **3** displays a Curie–Weiss behavior in the temperature range of 5–300 K (Fig. 12b). The effective magnetic moment of $6.07\mu_{\mathrm{B}}$ at 300 K is slightly larger than the one ($5.92\mu_{\mathrm{B}}$) expected for a high-spin $\mathrm{Mn}^{2+}$ ion ($d^5$) in octahedral environment. At 2 K, $\mu_{\mathrm{eff}}$ is decreased to $2.77\mu_{\mathrm{B}}$, indicating the antiferromagnetic interaction between Mn(II) centers. The $\chi_M - T$ plot of compound **3** exhibits a maximum at 3.0 K, which provides further evidence of the antiferromagnetic interaction between Mn(II) centers. Linear-fitting of the magnetic data in the range of 20–300 K according to Curie–Weiss law gave a Weiss constant ($\theta$) of –3.8 (2) K. The weak antiferromagnetic interactions between Mn(II) ions are expected due to the long Mn⋯Mn distances. The Mn(II) ions in the three-dimensional network of **3** are bridged by a phosphonate group and have Mn⋯Mn separations of 5.571(1) Å.

TGA curves of compound **1** show two main weight losses (Fig. 13). The compound is stable up to 287 °C. Then

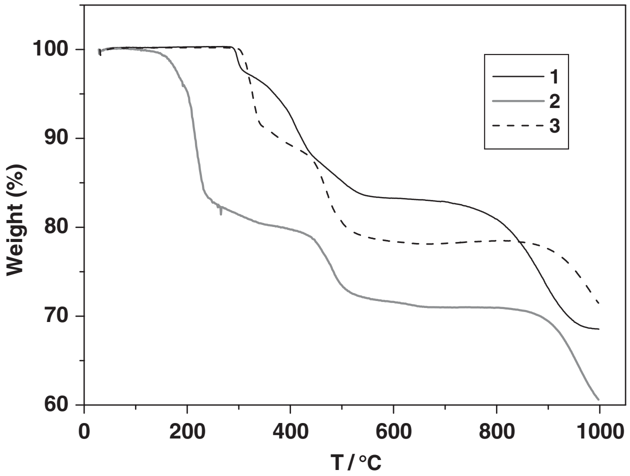

Fig. 13. TGA curves of compounds **1**–**3**.

it started to decompose from 287 °C and continued up to 600 °C with a weight loss of 17.1%, which corresponds to release of water molecules formed by the condensation of hydrogen phosphonate groups and the partial combustion of the organic group. The second weight loss from 720 to 1000 °C corresponds to the further combustion of the phosphonate ligand. The total weight loss at 1000 °C is about 31.5%. TGA curves for compound **2** show two main steps of weight losses. The first step starts at about 140 °C and is complete at 290 °C, which corresponds to the release of one lattice water molecule and two aqua ligands. The weight loss of 17.9% is in good agreement with the calculated value (17.1%). The second step covers a temperature range of 290 to 530 °C, which corresponds to release of water molecule formed by the condensation of hydrogen phosphonate groups and the partial pyrolysis of the organic group. The third weight loss from 830 to 1000 °C corresponds to the further combustion of the phosphonate ligand. The total weight loss at 1000 °C is about 39.5%. Compound **3** is stable up to about 290 °C. Then it starts to decompose in three stages. The first step (290–351 °C) with a weight loss of 7.04% corresponds to the loss of one aqua ligand (calculated value 6.53%). The second step is release of water molecules formed by the condensation of hydrogen phosphonate groups and the partial pyrolysis of the organic group, covering a temperature range from 351 to 580 °C. The third weight loss from 850 to 1000 °C corresponds to the further combustion of the phosphonate ligand. The total weight loss at 1000 °C is about 28.6%. For all three experiments, the final residuals are not identified due to their corrosion nature to our sample container ($Al_2O_3$ crucible). TGA analysis for compound **4** was not performed due to insufficient quantity of samples.

## 4. Conclusion

In summary, the hydrothermal syntheses and crystal structures of four new divalent metal aminodiphosphonates have been described. Although compounds **1**–**3** have a same $M/L$ ratio (1:1), they display completely different types of structures. Compound **1** has a linear chain structure, whereas compound **2** has a layer architecture built from $CoO_6$ octahedra bridged by phosphonate ligands. In compound **3**, the interconnection of the manganese(II) ions by bridging imino-diphosphonate ligands leads to the formation of 3D network. These structural differences lie in coordination numbers for the metal(II) ion, the aqua liagnds present and the coordination mode of phosphonate ligand adopts. Compound **4** has a pillar-layered structure, the layers composed of Cu(II) ions bridged by aminodiphosphonate ligands are interconnected by 4,4′-bipy ligands to form channels along *c*-axis. The structures of metal phosphonates are affected by many factors, such as the extent of deprotonation for the diphosphonate ligand, the nature of metal ion, the coordination-completing agents such as aqua ligand and other second ligand.

## Acknowledgments

We gratefully acknowledge the financial support from the National Natural Science Foundation of China (Project No: 20371074) and NSF of Fujian Province (No. E0420003).

## Appendix A. Supplementary data

Supplementary data associated with this article can be found in the online version at doi:10.1016/j.jssc.2005.10.015.

## References

[1] [a] G. Alberti, U. Costantino, in: J.M. Lehn (Ed.), Comprehensive Supramolecular Chemistry, Pergamon-Elsevier Science Ltd., London, 1996, p. 1;
[b] A. Clearfield, Metal phosphonate chemistry, in: K.D. Karlin (Ed.), Progress in Inorganic Chemistry, vol. 47, Wiley, New York, 1998, pp. 371–510 (and references therein);
[c] A. Clearfield, Cur. Opin. Solid State Mater. 6 (2002) 495.
[2] [a] P.Y. Feng, X.H. Bu, G.D. Stucky, Nature 388 (1997) 735;
[b] M.D. Lilley, D.A. Butterfield, J.E. Lupton, et al., Nature 422 (2003) 878.
[3] [a] A.K. Cheetham, G. Ferey, T. Loiseau, Angew. Chem. Int. Ed. 38 (1999) 3268;
[b] J. Zhu, X. Bu, P. Feng, G.D. Stucky, J. Am. Chem. Soc. 122 (2000) 11563;
[c] C.N.R. Rao, S. Natarajan, R. Vaidhyanathan, Angew. Chem. Int. Ed. 43 (2004) 1466.
[4] [a] F. Fredoueil, M. Evain, D. Massiot, M. Bujoli-Doeuff, P. Janvier, A. Clearfield, B. Bujoli, J. Chem. Soc., Dalton Trans. (2002) 1508;
[b] P. Rabu, P. Janvier, B. Bujoli, J. Mater. Chem. 9 (1999) 1323;
[c] S. Drumel, P. Janvier, M. Bujoli-Doeuff, B. Bujoli, J. Mater. Chem. 6 (1996) 1843.
[5] [a] N. Stock, Solid State Sci. 4 (2002) 1089;
[b] N. Stock, S.A. Ferey, G.D. Stucky, A.K. Cheetham, J. Chem. Dalton Trans. (2000) 4292;

[c] N. Stock, G.D. Stucky, A.K. Cheetham, Chem. Commun. (2000) 2277.
[6] [a] M. Riou-Cavellec, M. Sanselme, M. Nogues, J.M. Greneche, G. Ferey, Solid State Sci. 4 (2002) 619;
[b] M. Sanselme, M. Riou-Cavellec, J.M. Greneche, G. Ferey, J. Solid State Chem. 164 (2002) 354;
[c] M. Riou-Cavellec, M. Sanselme, N. Guillou, G. Ferey, Inorg. Chem. 40 (2001) 723;
[d] M. Riou-Cavellec, M. Sanselme, J.M. Greneche, G. Ferey, Solid State Sci. 2 (2000) 717;
[e] M. Riou-Cavellec, M. Sanselme, G. Ferey, J. Mater. Chem. 10 (2000) 745;
[f] F. Serpaggi, G. Ferey, Inorg. Chem. 38 (1999) 4741.
[7] [a] A. Distler, S.C. Sevov, Chem. Commun. (1998) 959;
[b] D.L. Lohse, S.C. Sevov, Angew. Chem. Int. Ed. 36 (1997) 1619.
[8] [a] B. Zhang, A. Clearfield, J. Am. Chem. Soc. 119 (1997) 2751;
[b] A. Clearfield, C.V.K. Sharma, B. Zhang, Chem. Mater. 13 (2001) 3099;
[c] J.-G. Mao, Z. Wang, A. Clearfield, Inorg. Chem. 41 (2002) 3713;
[d] H.L. Ngo, W. Lin, J. Am. Chem. Soc. 124 (2002) 14298.
[9] [a] J.-G. Mao, Z.-K. Wang, A. Clearfield, Inorg. Chem. 41 (2002) 6106;
[b] J.-G. Mao, Z.-K. Wang, A. Clearfield, New J. Chem. 26 (2002) 1010;
[c] J.-G. Mao, A. Clearfield, Inorg. Chem. 41 (2002) 2319;
[d] J.-L. Song, H.-H. Zhao, J.-G. Mao, K.R. Dunbar, Chem. Mater. 16 (2004) 1884;
[e] C. Lei, J.-G. Mao, Y.-Q. Sun, H.-Y. Zeng, A. Clearfield, Inorg. Chem. 42 (2003) 6157;
[f] B.-P. Yang, J.-G. Mao, Y.-Q. Sun, H.-H. Zhao, A. Clearfield, Eur. J. Inorg. Chem. 88 (2003) 4211.
[10] [a] R. Vivani, U. Costantino, M. Nocchetti, J. Mater. Chem. 12 (2002) 3254;
[b] S.J. Hartman, E. Todorov, C. Cruz, S.C. Sevov, Chem. Commun. (2000) 1213;
[c] G.B. Hix, D.S. Wragg, P.A. Wright, R.E. Morris, J. Chem. Soc. Dalton Trans. (1998) 3359.
[11] [a] J.-G. Mao, Z.-K. Wang, A. Clearfield, Dalton Trans. (2002) 4541;
[b] N. Choi, I. Khan, R.W. Matthews, M. McPartlin, B.P. Murphy, Polyhedron 13 (1994) 847;
[c] R. LaDuca, D. Rose, J.R.D. DeBord, R.C. Haushalter, C.J. O'Conner, J. Zubieta, J. Solid State Chem. 123 (1996) 408;
[d] V. Soghomonian, R. Diaz, R.C. Haushalter, C.J. O'Conner, J. Zubieta, Inorg. Chem. 34 (1995) 4460;
[e] Y. Wang, S.S. Bao, W. Xu, J. Chen, S. Gao, L.M. Zheng, J. Solid State Chem. 177 (2004) 1297.
[12] [a] B.I. Makaranets, T.N. Polynova, N.D. Mitrofanova, M.A. Porai-Koshits, J. Struct. Chem. 32 (1991) 94;
[b] J.-G. Mao, Z.-K. Wang, A. Clearfield, Inorg. Chem. 41 (2002) 2334;
[c] J.-G. Mao, Z.-K. Wang, A. Clearfield, Dalton Trans. 99 (2002) 4457;
[d] U. Costantino, M. Nocchetti, R. Vivani, J. Am. Chem. Soc. 124 (2002) 8428.
[13] [a] S.-M. Ying, J.-G. Mao, B.-P. Yang, Z.-M. Sun, Inorg. Chem. Commun. 10 (2003) 1319;
[b] Z.-M. Sun, J.-G. Mao, Y.-Q. Sun, H.-Y. Zeng, A. Clearfield, New J. Chem. 27 (2003) 1326;
[c] Z.-M. Sun, B.-P. Yang, Y.-Q. Sun, J.-G. Mao, A. Clearfield, J. Solid State Chem. 176 (2003) 62;
[d] J.-L. Song, J.G. Mao, Y.-Q. Sun, A. Clearfield, Eur. J. Inorg. Chem. (2003) 4218.
[14] H. Jankovics, M. Dashalakis, C.P. Raptopoulou, A. Terzis, V. Tangoulis, J. Giapintzakis, T. Kiss, A. Slifoglou, Inorg.Chem. 41 (2002) 3366.
[15] A. Turner, P.A. Jaffrès, E.J. MacLean, D. Villemin, V. Mckee, G.B. Hix, J. Chem. Soc. Dalton Trans. (2003) 1314.
[16] [a] A. Cabeza, S. Bruque, A. Guagliardi, A.G. Aranda, J. Solid State Chem. 160 (2001) 278;
[b] D. Kong, Y. Li, J.H. Ross Jr., A. Clearfield, Chem. Commun. (2003) 1720;
[c] D. Kong, L. Yang, O. Xiang, et al., Chem. Mater. 16 (2004) 3020.
[17] N. Stock, Solid State Sci. 4 (2002) 1089.
[18] B.-P. Yang, Z.-M. Sun, J.-G. Mao, Inorg. Chem. Acta 357 (2004) 1583.
[19] G.M. Sheldrick, Program SADABS, Universität Göttingen, 1995.
[20] G. M. Sheldrick, SHELXTL, Crystallographic Software Package, SHELXTL (Version 5.1), Bruker-AXS, Madison, WI, 1998.
[21] A.L. Spek, Platon: A Multi-purpose Crystallographic Tool, Utrecht University, Utrecht, The Netherlands, 2001.